KURENAI 紅

Kyoto University Research Information Repository

KYOTO UNIVERSITY

Title	FT-IR Studies on Molecular Structure and Orientation of a Liquid Crystal, 4'-n-Octyl-4-cyanobiphenyl (Commemoration Issue Dedicated to Professor Naokazu Koizumi on the Occasion of his Retirement)
Author(s)	Hayashi, Soichi; Kurita, Kazumi; Kimura, Noriyuki; Umemura, Junzo; Takenaka, Tohru
Citation	Bulletin of the Institute for Chemical Research, Kyoto University (1985), 63(3): 276-295
Issue Date	1985-11-25
URL	http://hdl.handle.net/2433/77111
Right	
Type	Departmental Bulletin Paper
Textversion	publisher

Kyoto University

FT–IR Studies on Molecular Structure and Orientation of a Liquid Crystal, 4'–n–Octyl–4–cyanobiphenyl

Soichi HAYASHI, Kazumi KURITA, Noriyuki KIMURA, Junzo UMEMURA, and Tohru TAKENAKA*

Fourier transform infrared spectra have been measured of a thermotropic liquid crystal, 4'-n-octyl-4-cyanobiphenyl (8CB), in the crystalline, smectic A and nematic liquid crystalline, and isotropic liquid phases. Spectral feature of 8CB was significantly changed at the crystal-smectic A transition temperature, while almost no change was observed at other transition temperatures. Interface-induced orientation and its temperature dependence were examined for 8CB in contact with KBr surfaces which have been treated in various ways such as rubbing and lecithin coating. The same studies were also carried out for free standing films. As the results of whole experiments, the four phases are found to be characterized by the orientation behaviours of molecules and its dependence on the history of thermal treatments.

KEYWORDS: FT-IR/ Molecular structure/ Orientation/ Surface/ 4'-n-Octyl-4-cyanobiphenyl/ Thermal process/ Free film/ Liquid crystal/

1. INTRODUCTION

Orientation behaviour of liquid crystals has drawn considerable attention because of their importance as display elements and relevance to biological membranes.[1-8] In a previous paper,[9] we measured the polarized FT-IR spectra of a trace of water dissolved in a thermotropic liquid crystal, 4'-n-octyl-4-cyanobiphenyl (abbreviated as 8CB) which was highly oriented in a magnetic field. The orientation of water was discussed in connection with that of 8CB.

In the present paper, molecular structure of 8CB and effect of the surface state of KBr windows on molecular orientation are studied in the crystalline, smectic A, nematic, and isotropic phases. Molecular orientation in free standing films was also examined. The dependence of orientation behaviours on thermal treatments was further studied to elucidate the relation between the intermolecular interactions of 8CB and the forces acting on the KBr and free surfaces.

2. CALCULATION PROCEDURE OF ORDER PARAMETER

It is known that there are two types of uniaxial orientations in liquid crystalline films: one is the homogeneous (planar) orientation in which the optical axis lies parallel to the film surface, the other is the homeotropic orientation where the optical axis is normal to the film surface. In the former case, the orientational order parameter S can be expressed as

*林 宗市, 栗田和実, 木村功之, 梅村純三, 竹中 亨: Laboratory of Surface Chemistry, Institute for Chemical Research, Kyoto University, Uji, Kyoto-fu 611.
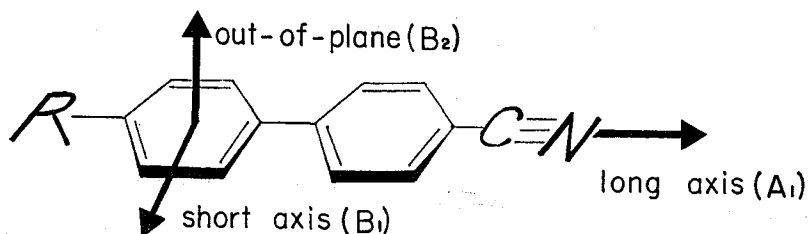
Fig. 1. Directions of the transition moments of the absorption bands which belong to the three infrared active species A_1, B_1, and B_2.

$$S = \frac{A_{\parallel} - A_{\perp}}{A_{\parallel} + 2A_{\perp}} \tag{1}$$

where, $A_{\parallel}$ and $A_{\perp}$ are the absorbances for the polarized radiation with electric vectors parallel and perpendicular to the optical axis of the uniaxial orientation, respectively.

In the case of homeotropic orientation, on the other hand, the dichroism can not be observed by the transmission spectra, because the optical axis is normal to the film surface. We have reported a simple method to determine the S-value for homeotropic films.[10] This is based on measurements of the infrared intensity ratio R of the band of the homeotropic film to that of randomly oriented film with the same thickness. The order parameter S is given by

$$S = 1 - R. \tag{2}$$

The shortcoming of this method is difficulty of accurate measurements of film thickness. In this paper, this difficulty is overcome by the use of the three characteristic infrared bands belonging to the A_1, B_1, and B_2 symmetry species of the cyanobiphenyl group (the point group C_{2v})whose transition moments are parallel to the long and short axes in the plane of the cyanobiphenyl group and normal to it, respectively[11,12] (Fig. 1). Those are the CN stretching band at 2230 cm^{-1} (the A_1 species), the combination band at 1915 cm^{-1} (the B_1 species) of the CH out-of-plane bending vibrations of the phenyl group, and its fundamental band at 815 cm^{-1} (the B_2 species). In the homeotropic system, the transition moments of the A_1, B_1, and B_2 species are uniformly distributed around the optical axis (Z axis) with angles of α, β. and γ, respectively, as shown in Fig. 2. Using the absorbances A_{α} and A_{α}' of the 2230 cm^{-1} band of the homeotropic system (thickness d) and the randomly oriented system (thickness d'), respectively, we have the order parameter S_{α} as

$$S_{\alpha} = 1 - \frac{A_{\alpha} d'}{A_{\alpha}' d} = 1 - R_{\alpha}\frac{d'}{d}, \tag{3}$$

where, $R_{\alpha} = A_{\alpha}/A_{\alpha}'$. Similarly, for the 1915 and 815 cm^{-1} bands, we have

$$S_{\beta} = 1 - R_{\beta}\frac{d'}{d}, \tag{4}$$

and

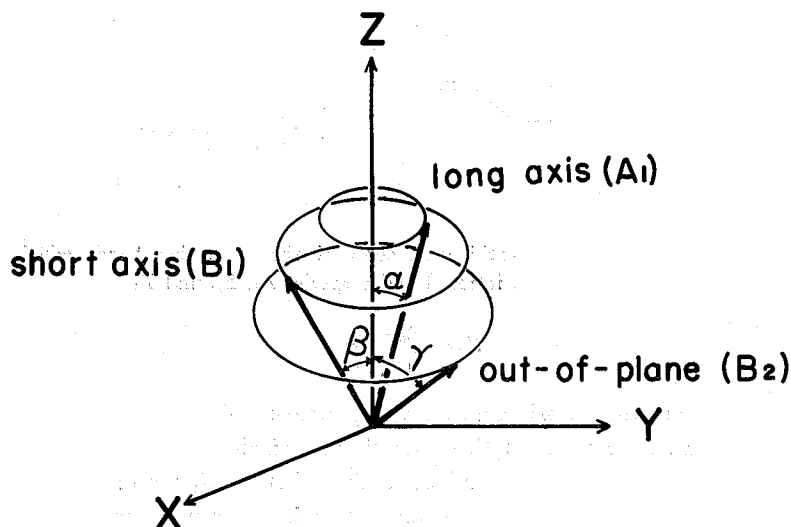$$S_{\gamma} = 1 - R_{\gamma}\frac{d'}{d}, \tag{5}$$

Fig. 2. Uniaxial orientation of the transition moments of the three characteristic bands belonging to the A_1, B_1, and B_2 species with respect to the Z (optical) axis.

respectively. Since the sum of the order parameters with respect to the three mutually perpendicular directions in a uniaxial system is zero,[9]

$$S_\alpha + S_\beta + S_\gamma = 3 - \frac{d'}{d}(R_\alpha + R_\beta + R_\gamma) = 0. \tag{6}$$

Thus we have

$$\frac{d'}{d} = \frac{3}{R_\alpha + R_\beta + R_\gamma}. \tag{7}$$

Therefore, the order parameters in the homeotropic system can be evaluated by Eqs. (3), (4), (5), and (7), without measuring the sample thickness.

3. EXPERIMENTAL

A sample of 8CB (purity 99.5%) was purchased from B.D.H. Chemicals Ltd., Great Britain. The transition temperatures were found to be 22, 34, and 40 °C for crystal-smectic A, smectic A-nematic, nematic-isotropic transitions, respectively. Egg yolk lecithin was purchased from Merck and used without further purification.

Samples were prepared in various ways.

Sample I: The KBr pellet of 8CB was prepared by the usual method (randomly oriented sample).

Sample II: Two KBr windows were rubbed unidirectionally by using a diamond paste with an average diameter of 1/4 μm. The 8CB sample was sandwiched between the KBr windows. A well oriented crystalline layer was carefully developed by cooling the sample from room temperature to about 0 °C with appropriate temperature gradient along the rubbing direction. Thus, the direction of crystal growth was parallel to the rubbing direction. The thickness of the sample was adjusted to be about 15 μm.

Sample III: A well oriented crystalline layer was developed similarly to Sample II, but the direction of crystal growth was perpendicular to the rubbing direction.

Sample IV: The 8CB sample was sandwiched between two KBr windows which had not been rubbed. A crystalline layer was developed similarly to Sample II in parallel to the surface of the KBr windows.

Sample V: The 8CB sample was sandwiched between two KBr windows which had been overcoated with lecithin by the method reported by Chatelste.[13] A crystalline layer was developed similarly to sample II in parallel to the surface of the KBr window.

Sample VI: The sample was sandwiched between two KBr windows which had been rubbed unidirectionally by a diamond paste. The temperature of the sample was initially increased up to 45°C (isotropic phase), and then decreased to about 20°C, a few degrees below T_{cs}. At this temperature the samples were supercooled. Infrared spectra were measured at various temperatures in heating process of this sample.

Sample VII: The sample was sandwiched between two KBr windows which had been overcoated with lecithin, and thermally treated in the similar way to Sample VI. Infrared measurements were carried out also in the same way as Sample VI.

Sample VIII: Free standing film was extended within a rectangular frame made of glass and teflon as shown in Fig. 3. Infrared spectra were measured at various temperatures on heating the sample from 20°C.

The samples thus prepared were mounted in a cell, whose temperature was controlled within ±0.1°C by circulating thermostated water. The temperature was monitored

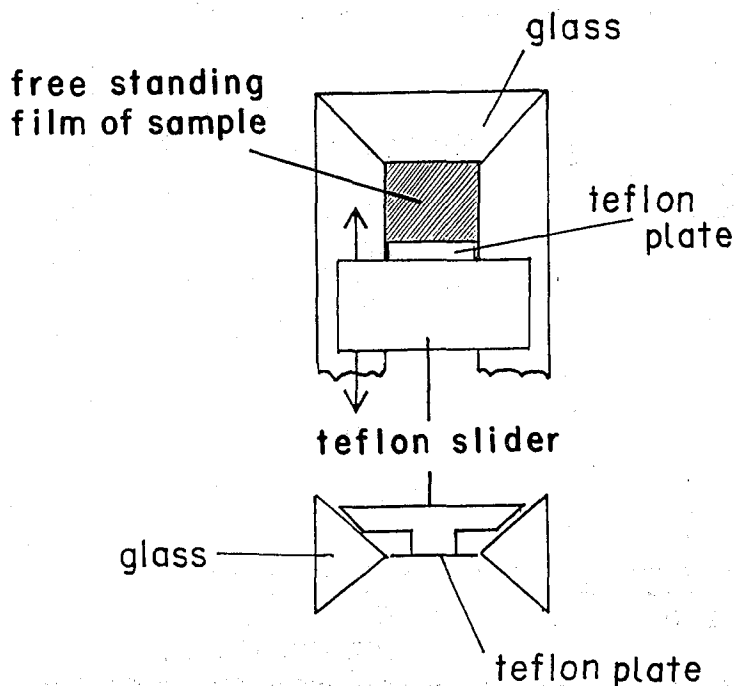Fig. 3. The rectangular frame for the free standing film.

S. HAYASHI, K. KURITA, N. KIMURA, J. UMEMURA, and T. TAKENAKA

by a copper-constantan thermocouple.

Infrared spectra were recorded on a Nicolet FT-IR spectrophotometer model 6000C equipped with an MCT detector. When necessary, a wire grid polarizer was used. The
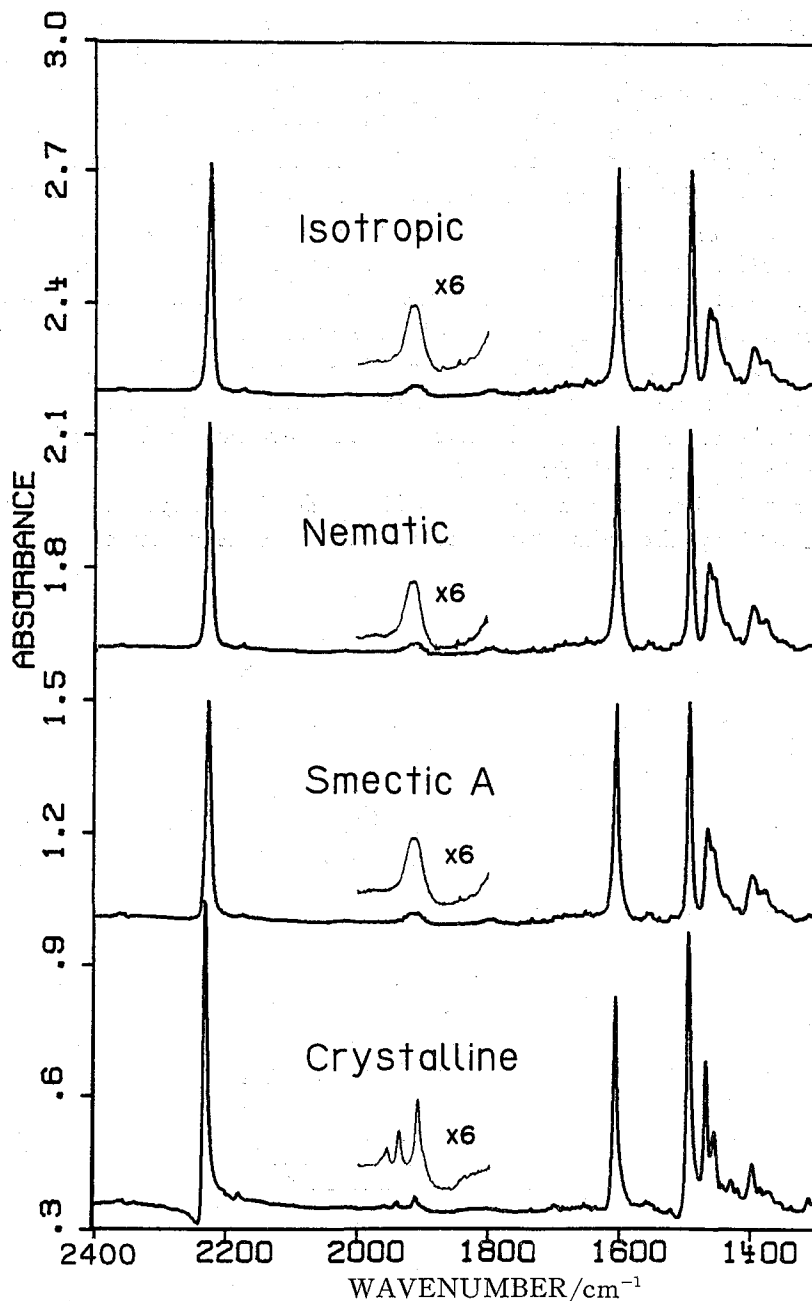

Fig. 4. The IR spectra in the range from 2400 to 1300 cm⁻¹ of 8CB in a KBr pellet in the crystalline, smectic A, nematic, and isotropic phases.

interferograms were accumulated 250 times by using a maximum optical retardation of 0.25 cm to yield a resolution of about 4 cm⁻¹ with high S/N ratio. The spectrophotometer was purged with dry air to eliminate atmospheric water and carbon dioxide.

4. RESULTS AND DISCUSSION

4.1. Infrared spectra of four phases

Figures 4 and 5 represent the infrared spectra in the frequency ranges of 2400-1300 and 1300-600 cm⁻¹, respectively, of 8CB in the KBr pellet (Sample I) in the crystalline,
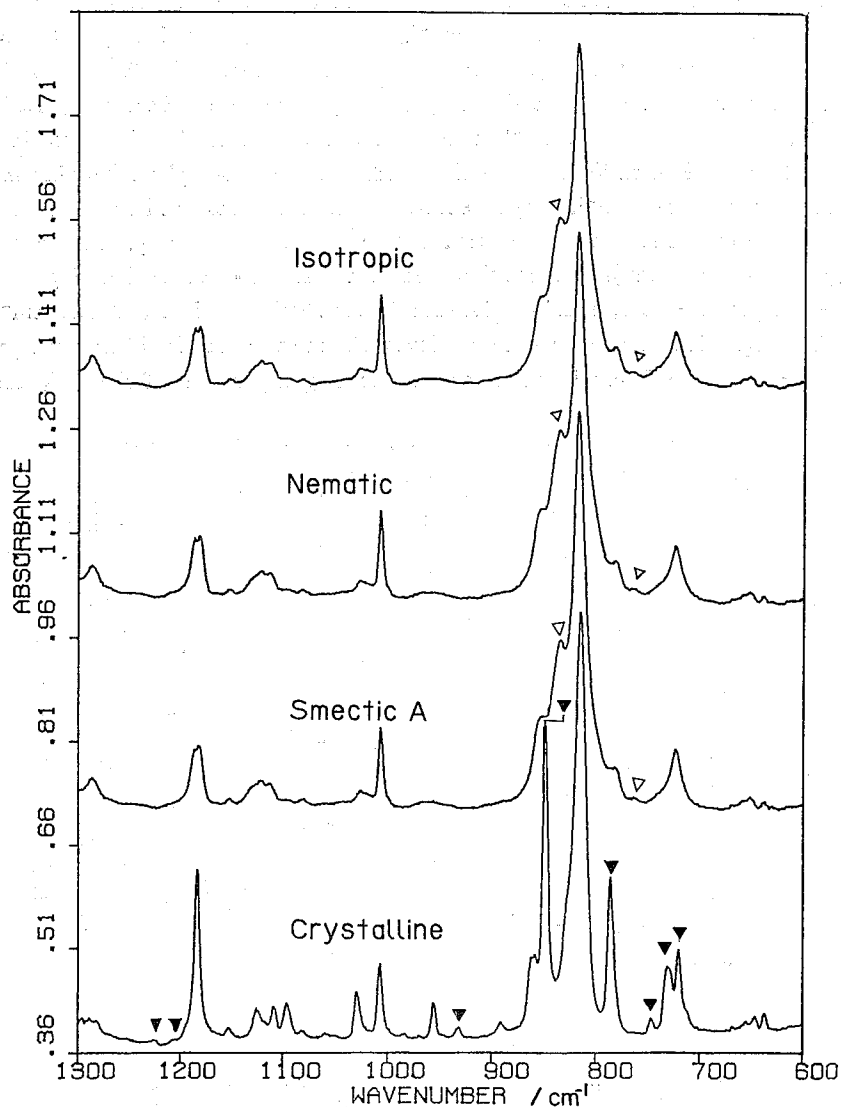

Fig. 5. The IR spectra in the range from 1300 to 600 cm⁻¹ of 8CB in a KBr pellet in the crystalline, smectic A, nematic, and isotropic phases.
▼ indicates absoption bands due to the *trans* zigzag conformation,
▽ indicates absorption bands due to the *gauche* conformation.

S. HAYASHI, K. KURITA, N. KIMURA, J. UMEMURA, and T. TAKENAKA

smectic A, nematic, and isotropic phases. As mentioned above, the absorption bands at 2230, 1915, and 815 cm^{-1} are assigned to the CN stretching vibration, the combination of the CH out-of-plane bending vibrations of the phenyl group, and its fundamental vibration, respectively. Besides these, there are the CC stretching bands of the phenyl group at 1608, 1496, and 1400 cm^{-1}, the CH$_2$ scissoring band at 1467 cm^{-1}, the CH in-plane bending band at 1184 cm^{-1}, the phenyl CCC bending band at 1006 cm^{-1}.

Spectral features are significantly changed for the following bands at the crystal-smectic A phase transition temperature (T_{CS}), but are scarcely changed at other transition temperatures. In the crystalline phase, the CH$_2$ rocking band of the octyl chain splits into two components at 719 and 730 cm^{-1}. The band progression due to the CH$_2$ rocking-twisting modes of the octyl chain are detected at 931, 850, 785, and 746 cm^{-1}, while the band progression due to the CH$_2$ wagging modes are observed at 1226, and 1208 cm^{-1}. The 850 and 785 cm^{-1} bands show strong absorption in crystalline state. These bands may be intensified by coupling with the CH out-of-plane bending mode of the phenyl group at 815 cm^{-1}. Large decreases in intensity observed for these bands in higher temperature phases may be caused by the distortion of the planar structure of the octyl chain, accompanying decoupling with the CH out-of-plane bending vibration. In these phases, the CH$_2$ rocking vibration is observed as a singlet at 723 cm^{-1}, and the band progressions almost disappear. Newly observed bands in higher temperature phases at 833 and 763 cm^{-1} are attributed to coupling modes of the CH$_3$ and CH$_2$
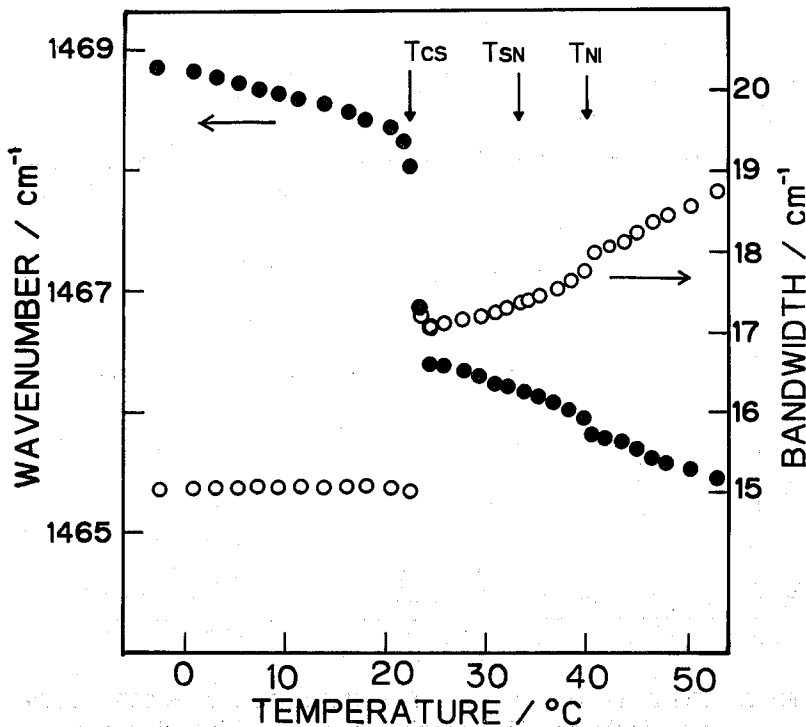

Fig. 6. Temperature dependence of the frequency (●) and the half-bandwidth (○) of the CH$_2$ scissoring band of 8CB in a KBr pellet.

rocking vibrations in the *gauche* conformation.[14] These findings suggest that in the crystalline phase, the hydrocarbon chain is in the planar *trans* zig-zag conformation with orthorhombic subcell packing, while in other phases, internal rotation occurs in the hydrocarbon chain providing the *gauche* conformation.

Temperature dependence of the frequencies and half-bandwidth of major bands of 8CB was examined. Typical results are shown in Fig. 6 for the CH_2 scissoring band. T_{CS}, T_{SN}, and T_{NI} denote the crystal-smectic A, smectic A-nematic, and nematic–isotropic phase transition temperatures, respectively. With increasing temperature, the band frequency abruptly decreases, and the bandwidth increases at T_{CS}, and both are followed by the gradual changes in the same directions at higher temperatures. This fact indicates that with increasing temperature the hydrocarbon chain packing becomes looser and the molecular motion becomes more vigorous at T_{CS} and then both change gradually at higher temperatures.

Figures 7 and 8 demonstrate the temperature dependences of the frequency and half-bandwidth of the CN stretching band and the CH out-of-plane bending band of the phenyl group, respectively. The CN stretching frequency largely decreases with increasing temperature at T_{CS} (Fig. 7), while the CH out-of-plane frequency increases
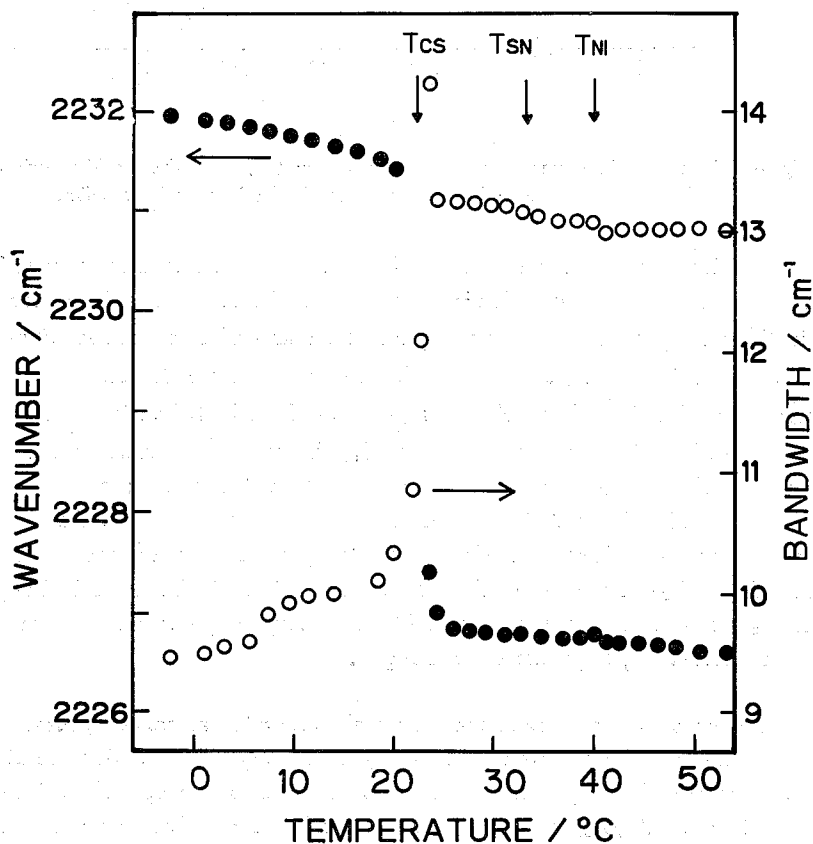

Fig. 7. Temperature dependence of the frequency (●) and the half-bandwidth (○) of the CN stretching band of 8CB in a KBr pellet.
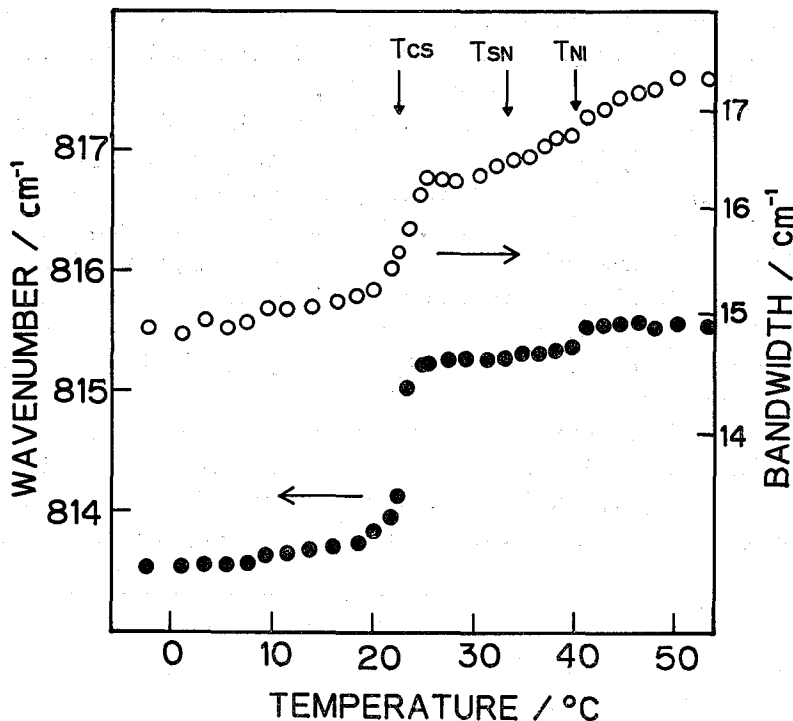
Fig. 8. Temperature dependence of the frequency (●) and the half-bandwidth (○) of the CH out-of-plane bending band of 8CB in a KBr pellet.

(Fig. 8). The direction of the frequency shift has been discussed in connection with the type of intermolecular interaction.[15] The changes in frequency is caused by the change in the arrangement of surrounding molecules around a particular vibrating molecule, and are obvious at T_{cs}. Since the bandwidth usually increases with increasing temperature, the direction of the change in bandwidth of both bands at T_{cs} and that of the CH out-of-plane bending band above T_{cs} is usual. However, that of the CN stretching band above T_{cs} is unusual. Gordon has studied a relation between the band shape and the rotational correlation function,[16] and suggested that the faster rotational motion results in the wider bandwidth. The temperature dependence observed on bandwidth above T_{cs} reveals that the rotational motion of the cyanobiphenyl group around its C_2 axis become more vigorous with increasing temperature, and the rotations around other axes being kept almost unchanged.

4.2. The direction of crystal growth and molecular orientation at various phases

We are discussing the orientation of the cyanobiphenyl group under the assumption of the C_{2v} symmetry of this group. Figure 9 demonstrates the temperature dependences of the dichroic ratio $A_{\parallel c}/A_{\perp c}$ in the logarithmic scale for the three characteristic bands at 2230 (A_1 species), 1915 (B_1 species), and 815 (B_2 species) cm^{-1} of Sample II. Here $A_{\parallel c}$ and $A_{\perp c}$ are the absorbances for the polarized radiations with the electric vectors
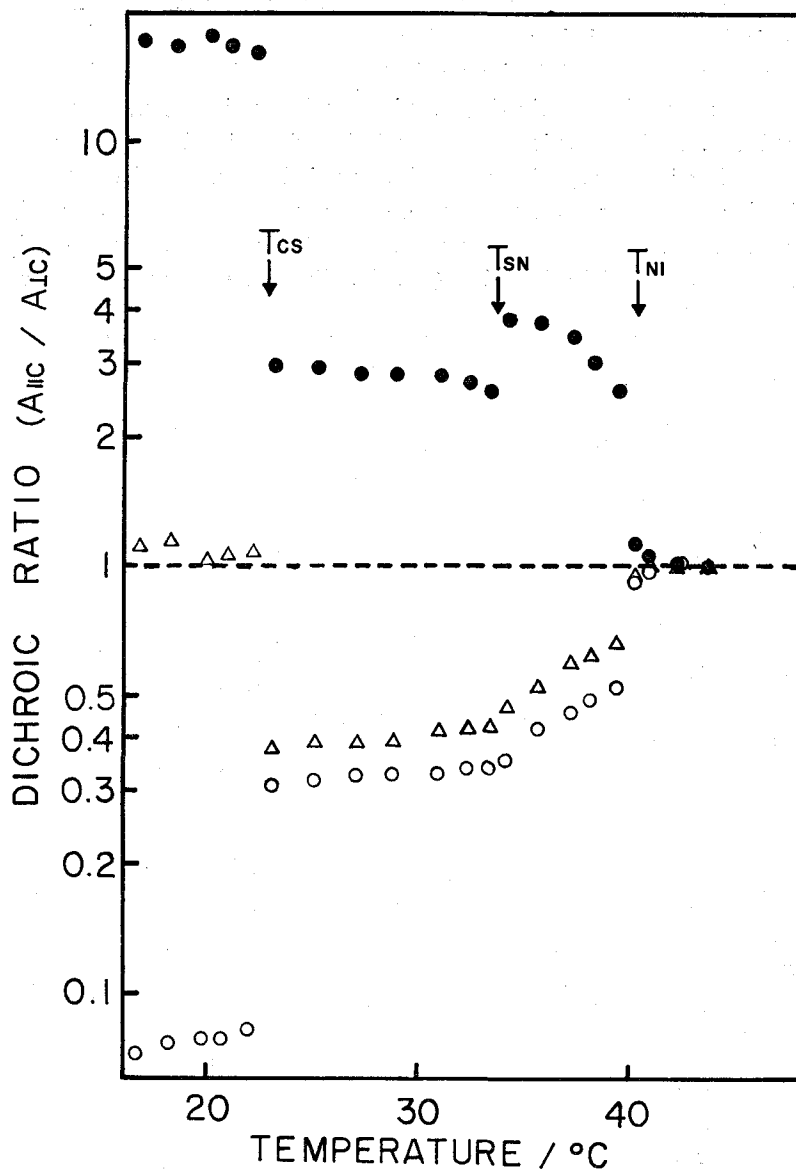
Fig. 9. Temperature dependence of the dichroic ratios for the 2230 (●), 1915 (△), and 815 cm⁻¹ (○) bands of Sample II.

parallel and perpendicular to the direction of crystal growth. The CN stretching band at 2230 cm⁻¹ shows large parallel dichroism in the crystalline state, indicating that the long axis of the cyanobiphenyl group is oriented almost parallel to the direction of crystal growth. The CH out-of-plane bending band at 815 cm⁻¹ exhibits large perpendicular dichroism. The combination band of the CH out-of-plane modes at 1915 cm⁻¹ is found to be weaker in this sample (the spectrum is not shown here) than in the randomly oriented sample (Sample I, Fig. 4) and shows no dichroism. These facts

indicate that the molecular plane is oriented parallel to the direction of crystal growth, and perpendicular to the window surface.

The parallel orientation of the long axis to the direction of crystal growth in the crystalline phase is still observed in the smectic A and nematic phases, although its degree is largely reduced. In the smectic A phase, uniaxial orientation is usually expected with respect to the direction of crystal growth. However, it is found to be not the case in this sample, because the sum of the three-S-values calculated from observed dichroic ratios of the characteristic bands by the use of Eq. (1) is found to be -0.15, instead of zero expected for uniaxial orientation (Eq. 6). Since the order parameter can be
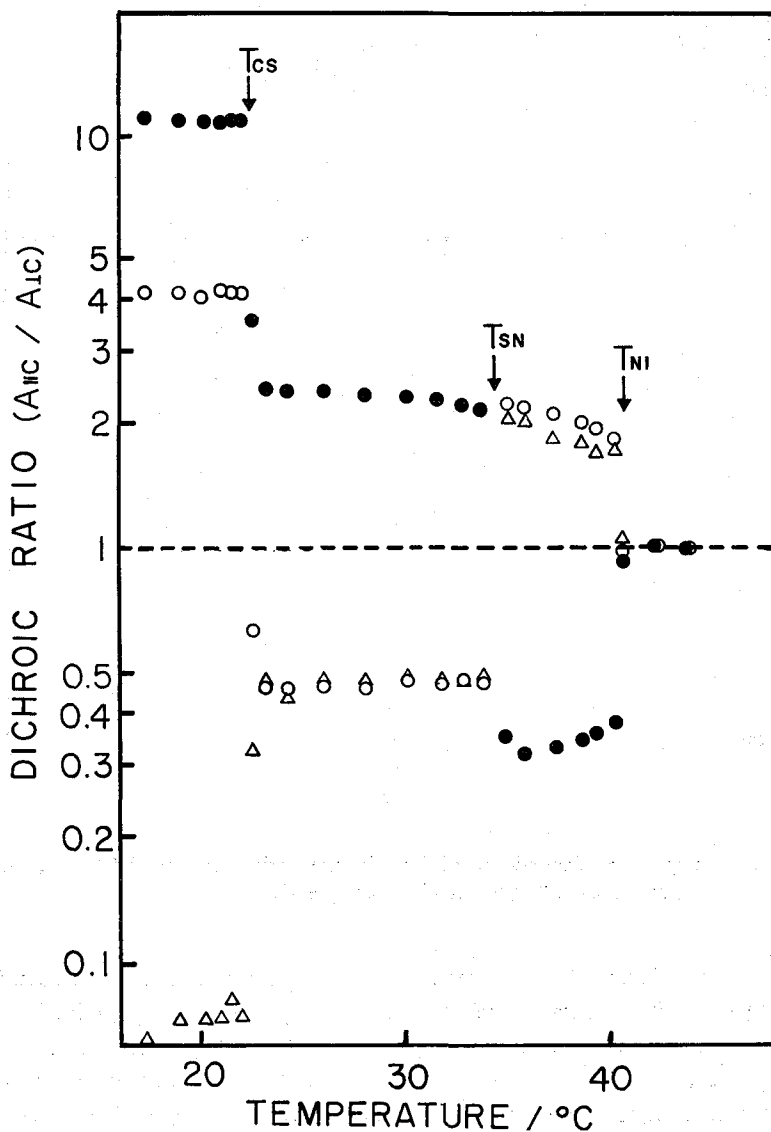

Fig. 10. Temperature dependence of the dichroic ratios of the 2230 (●), 1915 (△), and 815 cm^{-1} (○) bands of Sample III.

definded only for uniaxially oriented system, the molecular orientation of this sample is described in terms of the dichroic ratio instead of the order prarmeter in Fig. 9. In the nematic phase, the uniaxial orientation is obviously realized as is confirmed by the fact that the sum of S-values is zero ($S_\alpha \fallingdotseq 0.45$, $S_\beta \fallingdotseq -0.30$, $S_\gamma \fallingdotseq -0.15$). The large gap of the dichroic ratios for the 2230 cm^{-1} band at T_{SN} is caused by the change in the molecular orientation from non uniaxial to uniaxial. No dichroism and therefore random orientation of molecules is found in the isotropic phase as expected.

The temperature dependence of the dichroic ratios for the three bands of Sample III (Fig. 10) is different from that of Sample II (Fig. 9). Although the 2230 cm^{-1} band shows large parallel dichroism in the crystalline phase as in the case of Sample II, the 1915 cm^{-1} band shows large perpendicular dichroism. The 815 cm^{-1} band of this sample is weak as compared with that of Sample I and shows parallel dichroism. These facts indicate that the long axis orients nearly parallel (with slight inclination) to the direction of crystal growth, and the molecular plane orients almost parallel to the window surface. In the both cases of Samples II and III, the long axis are parallel to the direction of crystal growth, irrespective of the rubbing direction, but the orientation about the long axis is different for each sample. The parallel orientation of the long axis in the crystalline phase still remains in the smectic A phase. The molecular orientation is also found to be not uniaxial. At T_{SN}, drastic changes in dichroisms occur. The 2230 cm^{-1} band gives rise to the change from parallel to perpendicular dichroism and 1915 and 815 cm^{-1} bands give rise to the change from perpendicular to parallel dichroism. This fact indicates that the long axis of the molecules turns from the direction of crystal growth to the rubbing direction at T_{SN}. In the nematic phase, S_α, S_β, and S_γ are calculated as 0.45, -0.30, and -0.15, respectively. The sum of them is equal to zero, indicating uniaxial orientation.

The temperature dependence on the dichroic ratios for Sample IV, which is not shown here, is quite similar to that for Sample II (Fig. 9). The long axis of the molecule orients parallel to the direction of crystal growth in the crystalline, smectic A, and nematic phases.

Figure 11 displays the dichroic ratios at various temperatures for Sample V. In the crystalline state, the 2230 cm^{-1} band shows large paralell dichroism, indicating that the long axis orients parallel to the direction of crystal growth. The 1915 cm^{-1} band shows large parpendicular dichroism as in the case of Sample III (Fig. 10). The 815 cm^{-1} band is observed to be very weak as compared with that of Sample I, suggesting that the direction of the transition moment of this band is almost normal to the window surface. In Fig. 11, this band shows larger parallel dichroism than the 2230 cm^{-1} band. Since, however, in this case dichroism of this band is very sensitive to the small inclination of the molecular plane, the orientation of the molecule is more or less the same as that of Sample III (Fig. 10). As in the case of Samples II, III, and IV, the parallel orientation of the long axis persistes in the smectic A phase, although the mangitude is largely reduced. In the nematic phase, no dichroism is observed. Because the intensity of the 2230 cm^{-1} band of this sample is much weaker than that of randomly oriented sample (Sample I), while the 1915 and 815 cm^{-1} bands belonging to the B_1 or B_2 species have comparatively strong absorption, the long axis of the molecule is though to
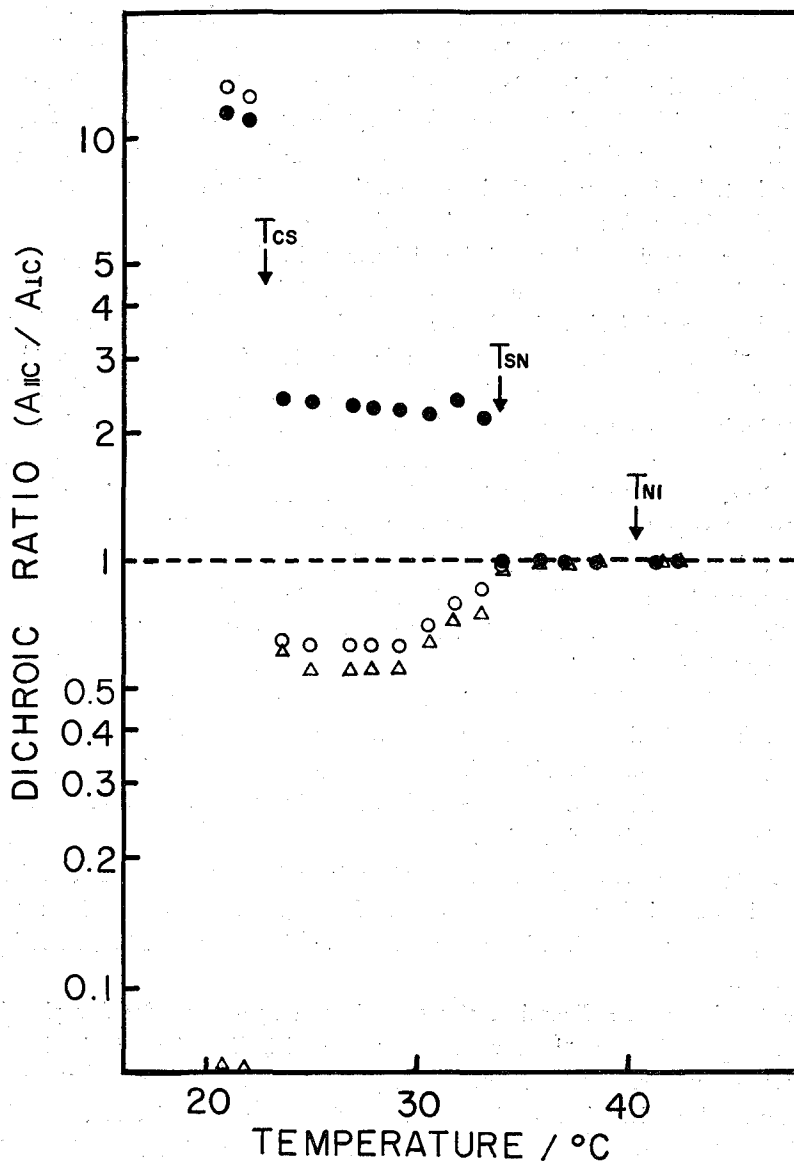
Fig. 11. Temperature dependence of the dichroic ratios of the 2230 (●), 1915
(△), and 815 cm^{-1} (○) bands of Sample V.

orient perpendicular to the window surface. In other words, the homeotropic orientation
is performed in the nematic phase. This was further confirmed by means of polarized
microscope. When the sample was placed between two crossed polarizer, it appeared
dark.[2] Similar results were obtained for the 8CB sample sandwiched between two KBr
windows which have been first rubbed by a diamond paste and then coated with leci-
thin. The effect of rubbing may be screened by the lecithin overcoat in this case.

　The results described in this section are schematically summarized in Fig. 12. The
thermal process, i. e., the history of thermal treatment, is shown at the top of the figure.

Thermal process

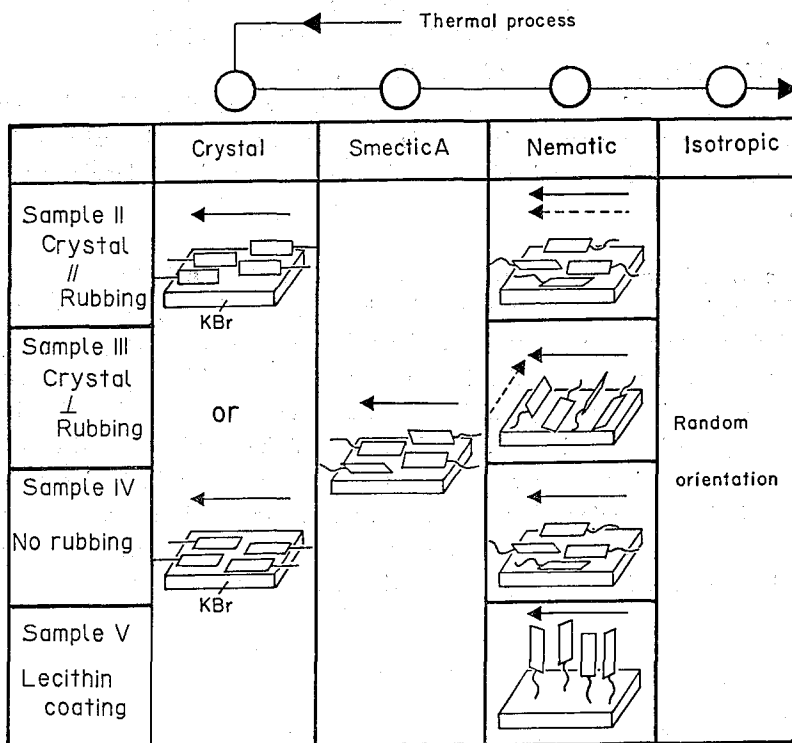|	Crystal	Smectic A	Nematic	Isotropic
Sample II Crystal // Rubbing	KBr			
Sample III Crystal ⊥ Rubbing	or			Random
Sample IV No rubbing	KBr			orientation
Sample V Lecithin coating				

Fig. 12.   Schematic illustration of orientation behaviour of 8CB in contact with KBr surfaces which have been treated in various ways. The samples were first crystallized and infrared spectra were measured in crystalline, smectic A, nematic, and isotropic phases on the process of sample heating. ⟵— indicates the direction of crystal growth, and ⟵--- indicates the rubbing direction.

The samples were crystallized at first, and their FT-IR spectra were measured in this phase and then in smectic A, nematic, and isotropic phases on the process of sample heating. The molecular orientation in the crystalline phase is determined exclusively by the direction of the temperature gradient in the crystal growth, and is independent of the state of the window surface with which the sample is in contact. Namely, the long axis of the molecule always orients parallel to the direction of crystal growth. The orientation around the long axis seems to be determined depending upon the orientation of a seed crystal first obtained. The parallel orientation of the long axis of the molecule in the crystalline phase remains in the smectic A phase, while the rotation around the long axis is considerably activated. The molecular orientation is still not uniaxial. In this case, two types of force may be considered: one is the intermolecular force which acts so as to remain the molecular orientation unchanged, and the other is the surface force which acts so as to determine the molecular orientation depending on the state of the window surface. It seems that in the smectic A phase, the intermolecular force is predominant. In the nematic phase, on the other hand, the surface force surpasses the intermolecular force, and the orientation of the long axis depends on the state of the

S. HAYASHI, K. KURITA, N. KIMURA, J. UMEMURA, and T. TAKENAKA

window surface. Namely, the long axis orients parallel to the rubbing direction in Samples II and III. This results in the turning of the long axis from direction of crystal growth to the rubbing direction at T_{SN} of Sample III. In Sample V, the long axis orients perpendicular to the window surface. In sample IV, where the KBr windows are not rubbed, the molecules behave as in Sample II. The molecular orientation is uniaxial in this phase for all samples examined. In the isotropic phase, the molecules are randomly oriented.

4.3. Molecular orientation in the sample prepared without crystallization

In this section, the molecular orientation in Samples VI, VII, and VIII are discussed. Figure 13 demonstrates the temperature dependence of the order parameters in the homogeneous system of Sample VI. The order parameters with respect to the rubbing direction were obtained from the dichroic ratios of the three bands belonging to the A_1, B_1, and B_2 species by using Eq. (1). The sum of the S-values for the three bands is equal to zero both in the smectic A and the nematic phases, indicating that the system is in uniaxial orientation. Three order parameters gradually approach to zero with increasing temperature. The temperature dependence of the order parameter of the long axis in the nematic phase agree well with that reported by Karat and Mudhusu-
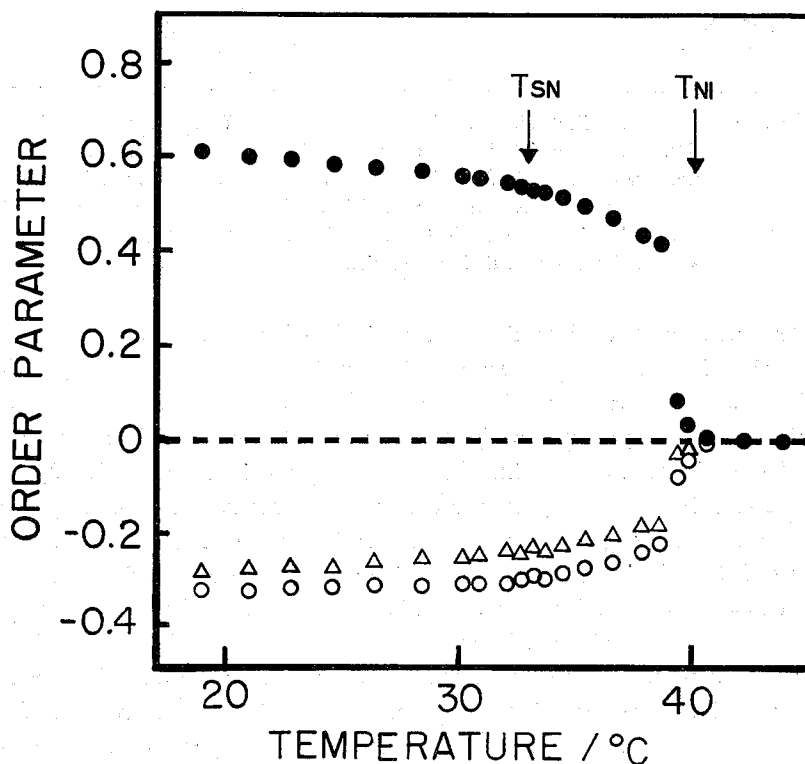

Fig. 13. Temperature dependence of the orientational order parameters with respect to the rubbing direction for the 2230 (●), 1915 (△), and 815 (○) cm⁻¹ bands of Sample VI.
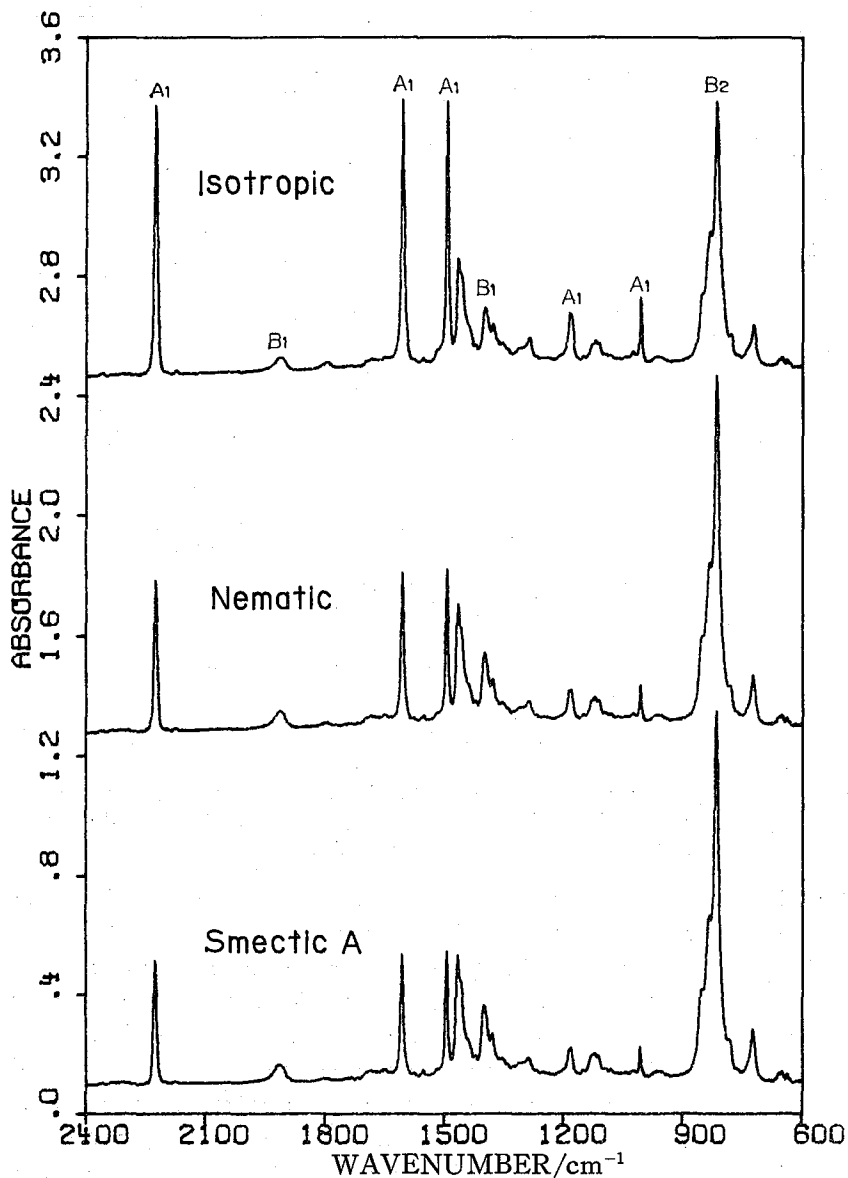
Fig. 14. IR spectra in the range from 2400 to 600 cm^{-1} of 8CB in a homeotropic system of Sample VII.

dana[17] who obtained the order parameter from the refractive indexes. At T_{NI}, the order parameters become zero.

Figure 14 displays the infrared spectra of 8CB in a homeotropic system of Sample VII. The absoption bands at 2230, 1608, 1496, and 1184 cm^{-1} which are classified into the A_1 symmetry species increase their intensities in the order of the smectic A, nematic, and isotropic phases, while the B_1 bands at 1915 and 1400 cm^{-1}, and the B_2 bands at 815 cm^{-1} decrease their intensities in the same order. These facts reveal that the
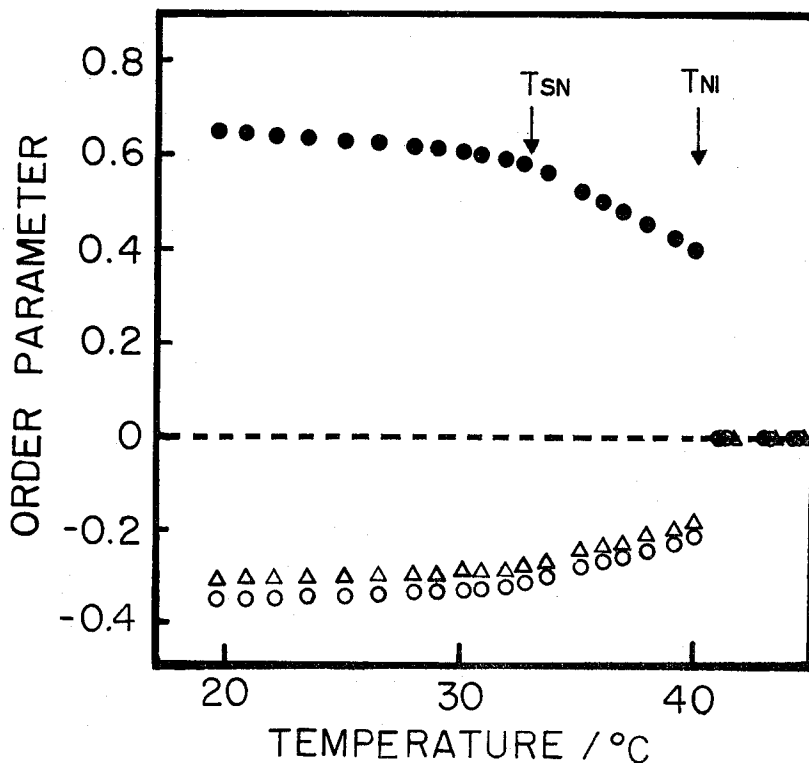
Fig. 15. Temperature dependence of the orientational order parameters with
respect to the normal to the surface for the 2230 (●), 1915 (△),
and 815 (○) cm^{-1} bands of Sample VII.

molecular orientation is deteriorated with increasing temperature. This is quantitatively
shown by the temperature dependence of the order parameters (Fig. 15) which were
obtained from the intensity ratios R_α, R_β, and R_γ for the three characteristic bands at
2230, 1915, and 815 cm^{-1} by using the Eqs. (3), (4), (5), and (7). The order parameter
for this homeotropic system is almost the same as that for the homogeneous system
(Fig. 13). In the isotropic phase, order parameters become zero.

Figure 16 shows the temperature dependence of the order parameters around the
surface normal in a free standing film of Sample VIII. The order parameters for this
system are obtained by the same way as in the case of Sample VII. The temperature
dependence of the order parameters is found to be almost the same as that in Sample
VII in the smectic A phase, but fluctuates in the nematic phase. The reason of this
fluctuation is uncertain at present.

The results in this section are illustrated in Fig. 17, where the thermal process is
shown at the top of the figure. Samples were gradually cooled down from the isotropic
phase to the smetic A phase without crystallization. The FT-IR spectra are measured
in the smectic A, nematic, and isotropic phases on the process of sample heating. The
molecular orientation depends on the state of the window surface in Samples VI and
VII. The orientation of the long axis is parallel to the surface in the former sample,
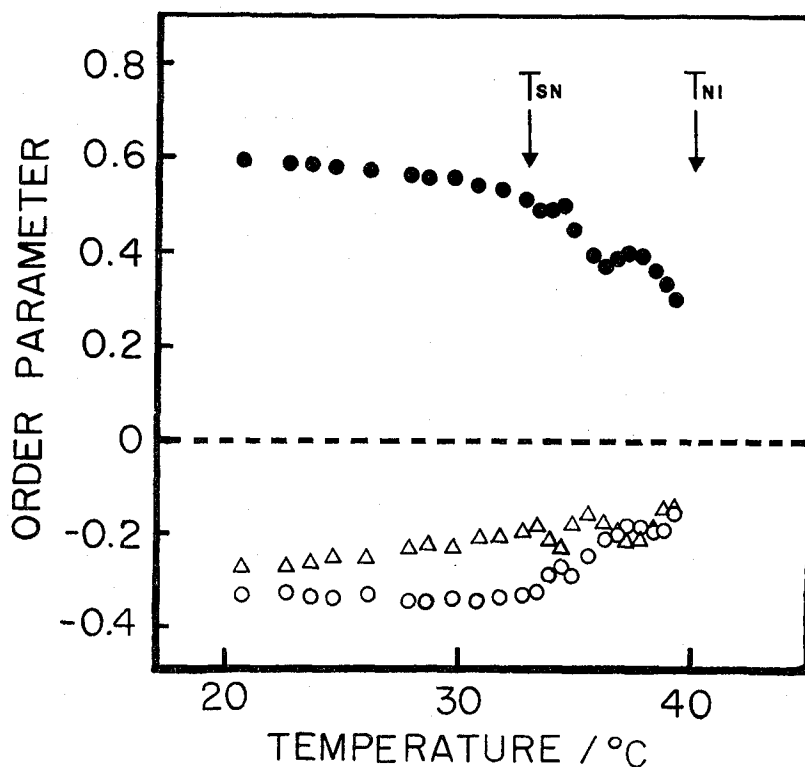while perpendicular in the latter sample. In Sample VIII, the molecule orients almost

(292)

Fig. 16. Temperature dependence of the orientational order parameters with respect to the normal to the surface for the 2230 (●), 1915 (△), and 815 (○) cm⁻¹ bands of Sample VIII.

perpendicular to the film surface. The uniaxial orientation occurs both in the smectic A and nematic phases for all the samples. The molecule can fluctuate only in the free surface. The force acting on the free surface seems to be weaker than that acting on the KBr surfaces. The order parameters gradually decrease with increasin temperature.

5. CONCLUSION

In Samples I to V, molecular structure dramatically changes at T_{CS}, but scarcely at T_{SN}, and T_{NI}. The alkyl chains are in the *trans* zig-zag form in the crystalline phases, but may rotate about C-C bonds to provide the *gauche* form in the smectic A, nematic, and isotropic phases. This rotational motion increases with increasing temperature.

It can be concluded that the four phases of 8CB are characterized by the orientation behaviour of the molecules as well as its dependence on the thermal process as follows. In the crystalline phase, the long axis of the molecule always orients parallel to the direction of crystal growth, but the orientation about the long axis is determined depending on the orientation of a seed crystal first obtained.

In the smectic A phase, it is interesting to compare the molecular orientation between Sample II in Fig. 12 and Sample VI in Fig. 17 (in both samples, the KBr windows are rubbed) and between Sample V in Fig. 12 and Sample VII in Fig. 17 (in both
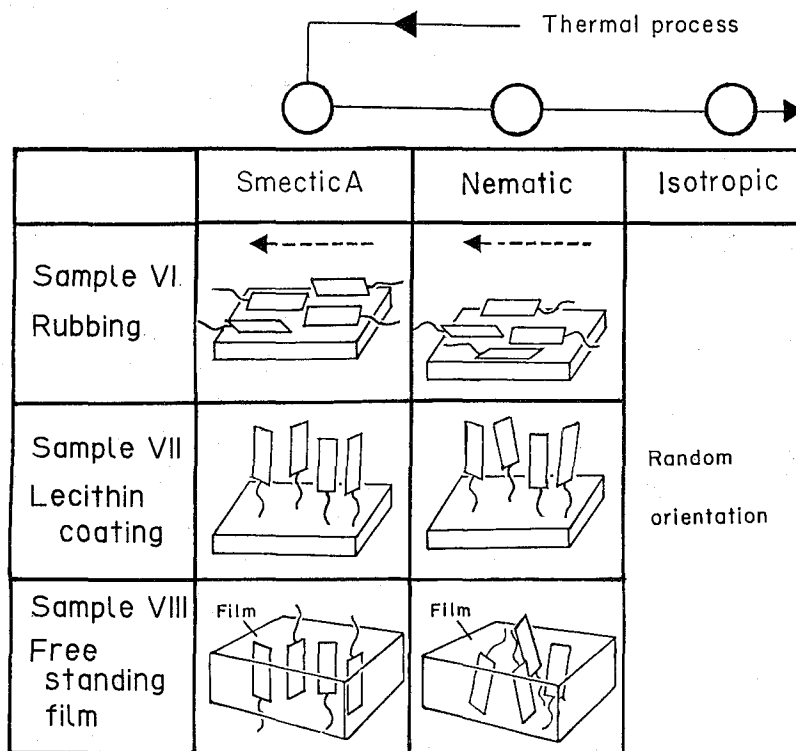
S. HAYASHI, K. KURITA, N. KIMURA, J. UMEMURA, and T. TAKENAKA

Fig. 17. Schematic illustration of orientation behaviour of 8CB for Samples VI, VII, and VIII, The samples were gradually cooled down from the isotropic phase to the smectic A phase without crystallization. Infrared spectra were measured in the smecic A, nematic, and isotropic phases on the process of sample heating. ←--- indicates the rubbing direction.

samples, the KBr windows are lecithin coated). In the case of Sample II and Sample VI, the long axis of the molecule is oriented parallel to the window surface. In the case of Sample V and Sample VII, however, the long axis is oriented parallel to the window surface in the former sample, but it is oriented perpendicular to the surface in the latter sample. All of these findings can be understood by an idea that the molecular orientation in the smectic A phase is determined by that in the previous phase of the thermal process, which is the crystalline phase for Samples II and V, but the nematic phase for Samples VI and VII. In the crystalline phase of Samples II and V, the long axis orients parallel to the crystal growth (the window surface). In the nematic phase of Sample VI, the long axis orients parallel to the rubbing direction (the window surface), but in the nematic phase of Sample VII, it orients perpendicular to the window surface. Thus it is likely that the intermolecular force plays an important role in the molecular orientation in the smectic A phase.

It is apparent in the nematic phase that the molecular orientation in Sample II and that in Sample VI are identical (parallel to the window surface) in each other. Further

the orientation in Sample V and that in Sample VII are also the same (perpendicular to the window surface) with each other. These facts reveal that the molecular orientation in the nematic phase is determined by the state of the window surface, and independent of the orientation in the previous phase of the thermal process. It can be said therefore that the surface force surpasses the intermolecular force in the nematic phase.

REFERENCES

(1) S. Jen, N. A. Clark, P. S. Pershan, and E. B. Priestley, *J. Chem. Phys.*, **66**, 4635 (1977).
(2) S. Featti, and L. Fronzoni, *Solid State Commun.*, **25**, 1087 (1978).
(3) A. Hatta, *Bull. Chem. Soc. Jpn.*, **50**, 2522 (1977).
(4) D. W. Berreman, *Phys. Rev. Letters*, **28**, 1683 (1972).
(5) F. Kahn, G. Taylor, and H. Schonhorn, *Proc. IEEE*, **61**, 823 (1973).
(6) K. Hiltrop, and H. Stegemeyer, *Ber. Bunsenges. Phys. Chem.*, **82**, 884 (1978).
(7) T. Uchida, K. Ishikawa, and M. Wada, *Mol. Cryst. Lig. Cryst.*, **60**, 37 (1980).
(8) T. Uchida, M. Ohgawara, and Y. Shibata, *Mol. Cryst. Liq. Cryst.*, **98**, 149 (1983).
(9) N. Kimura, J. Umemura, S. Hayashi, and T. Takenaka, *J. Mol. Struct.*, **116**, 153 (1984).
(10) N. Kimura, S. Hayashi, and T. Takenaka, *Bull. Inst. Chem. Res. Kyoto Univ.*, **58**, 559 (1980).
(11) Y. Kakiuchi, *Nippon Kagaku Zasshi*, **77**, 1839 (1956) ; **80**, 28 ; 250 ; 356 (1956).
(12) S. Hayashi, *Nippon Kagaku Zasshi*, **85**. 186 (1964).
(13) P. Chatelste, *Bull. Soc. Franc. Mineral. Cryst.*, **66**, 105 (1943).
(14) G. Zerbi, R. Magni, M. Gussoni, K. H. Moritz, A. Blogotto, and S. Dirlikov, *J. Chem. Phys.*, **75**, 3175 (1981).
(15) A. D. Buckingham, *Trans. Faraday Soc.*, **56**, 753 (1960).
(16) R. G. Gordon, *J. Chem. Phys.*, **43**, 1307 (1965).
(17) P. P. Karat and N. N. Madhusudana, *Mol. Cryst. Liq. Cryst.*, **36**, 51 (1976).